Dalton Transactions

Chiroptical switching behavior of heteroleptic ruthenium complexes bearing acetylacetonato and tropolonato ligands

Journal:	*Dalton Transactions*
Manuscript ID	DT-ART-08-2021-002592.R1
Article Type:	Paper
Date Submitted by the Author:	09-Sep-2021
Complete List of Authors:	Yoshida, Jun; Nihon University College of Humanities and Sciences, Chemistry Yamazaki, Kana; Kitasato University - Sagamihara Campus Tateyama, Kazunori; Kitasato University School of Science Graduate School of Science Yuge, Hidetaka; Kitasato University, Department of Chemistry, School of Science Sato, Hisako; Ehime University, Department of Chemistry

ARTICLE

Chiroptical switching behavior of heteroleptic ruthenium complexes bearing acetylacetonato and tropolonato ligands

Received 00th January 20xx,
Accepted 00th January 20xx

DOI: 10.1039/x0xx00000x

Jun Yoshida,*[a] Kana Yamazaki,[b] Kazunori Tateyama,[b] Hidetaka Yuge,[b] and Hisako Sato[c]

Four types of tris-chelate ruthenium complexes bearing acetylacetonato (acac) and tropolonato (trop) ligands were synthesized and optically resolved into Δ and Λ isomers: [Ru(acac)$_3$] (**Ru-0**), [Ru(acac)$_2$(trop)] (**Ru-1**), [Ru(acac)(trop)$_2$] (**Ru-2**), and [Ru(trop)$_3$] (**Ru-3**). The chiral HPLC chromatograms, electronic circular dichroism (ECD), and vibrational circular dichroism (VCD) of the four ruthenium complexes were systematically investigated. As a result, the absolute configurations of newly prepared enantiomeric complexes **Ru-2** and **Ru-3** were determined. For the case of **Ru-2**, its absolute configuration was also confirmed by single crystal X-ray diffraction analysis. The ECD changes upon chemical oxidation were further investigated for the four complexes. The ECD change of enantiomeric **Ru-1** was observed upon oxidation, whereas the oxidized species soonly returned to the neutral state within a few minutes. Enantiomers of **Ru-3** also showed explicit ECD changes upon oxidation. Further, the lifetime of the oxidized state was the longest among the four investigated complexes, whereas they racemized in solution at room temperature. In contrast, the enantiomers of heteroleptic complexes (**Ru-1** and **Ru-2**) concurrently exhibited ECD changes, relatively long lifetime of the oxidized state, and non- or quite slow racemization behavior. The co-existence of acac and trop ligands were the key to make the competing factors compatible in the resultant ruthenium complexes.

Introduction

Tris-chelate metal complexes such as [M(acac)$_3$] and [M(bpy)$_3$]$^{2+}$ (M = metal ions, acac=acetylacetonate, bpy=2,2'-bipyridine) have been actively investigated in terms of the electrochemical properties such as reversible and multi-step redox behaviors,[1–12] photoluminescence,[13–16] catalysts,[17,18] and ΔΛ chirality.[19–22] The combination of the redox and ΔΛ chiral properties is further fascinating from the viewpoint of chiroptical switching materials;[23–26] pioneering works were reported on the electronic circular dichroism (ECD) changes of [M(acac)$_3$] and [Ru(bpy)$_3$] derivatives upon the electrochemical oxidation.[27–29] However, tris-chelate metal complexes are still minor as a chiroptical switching material. Major coordination compounds that show chiroptical switching behaviors are those with different coordination geometries depending on the oxidation states; for example a copper complex, which favors tetrahedral and square pyramidal geometries in mono- and di-valent states respectively, is reported to show drastic chiroptical changes upon redox reactions.[30]

Our research group has investigated the electrochemical behavior of [Ru(trop)$_3$] (Htrop = tropolone) derivatives as a [Ru(acac)$_3$] analog.[31–33] Although trop is known to behave as an acac-like chelate ligand,[34] it can show different electronic states in the resultant metal complexes.[35] Tropolone can be regarded as a seven-membered analog of redox-active dioxolene, a collective name for catechol, semiquinone, and quinone.[36–41] We recently reported that cationic charge in mono-oxidized [Ru(trop)$_3$]$^+$ complex is distributed over the entire complex due to the mixing of frontier orbitals of a ruthenium ion and tropolonato ligands,[33] while the redox of [Ru(acac)$_3$] (acac = acetylactonate) relatively occurs at metal-based orbitals. [Ru(trop)$_3$] and its derivatives are hence expected to exhibit more drastic chiroptical changes upon redox. However, the chiral properties of [Ru(trop)$_3$] derivatives are hardly reported. Even the absolute configuration of enantiomeric [Ru(trop)$_3$] is not yet determined.

Motivated by the potential combination of redox and ΔΛ chirality in ruthenium tropolonato complexes, we in this study examined the systematic comparison of optically active [Ru(acac)$_3$] (**Ru-0**), [Ru(acac)$_2$(trop)] (**Ru-1**), [Ru(acac)(trop)$_2$] (**Ru-2**), and [Ru(trop)$_3$] (**Ru-3**) (Scheme 1). The electronic circular dichroism (ECD) and vibrational circular dichroism (VCD) spectra of the four ruthenium complexes were systematically investigated. As a result, the absolute configuration of **Ru-3** was determined, assisted by the DFT calculations. Finally, the ECD changes of these compounds were investigated upon oxidation by using ceric(IV) ammonium nitrate (CAN) as an oxidant.

[a] *Department of Chemistry, College of Humanities & Sciences, Nihon University, 3-25-40 Sakurajosui, Setagaya-ku, Tokyo 156-8550, Japan.*
[b] *Department of Chemistry, School of Science, Kitasato University, 1-15-1 Kitasato Minami-ku, Sagamihara, 252-0373, Japan.*
[c] *Graduate School of Science and Engineering, Ehime University, 2-5 Bunkyo-chou, Matsuyama, Ehime 790-8577, Japan.*

Electronic Supplementary Information (ESI) available: [MS spectrum and X-ray analysis data of **Ru-2**, chromatograms in the optical resolution, ECD, VCD and IR spectra, and time-dependent changes of UV-vis absorption]. See DOI: 10.1039/x0xx00000x

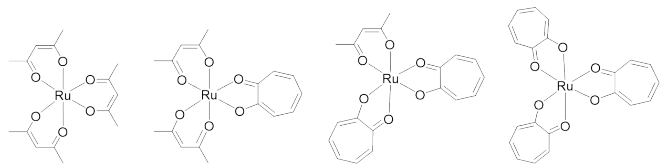

[Ru(acac)$_3$] (**Ru-0**) [Ru(acac)$_2$(trop)] (**Ru-1**) [Ru(acac)(trop)$_2$] (**Ru-2**) [Ru(trop)$_3$] (**Ru-3**)

Scheme 1 Four metal complexes investigated in this study.

Experimental

Physical measurements: ^{1}H NMR spectra were recorded at 600 MHz with a Bruker AVANCE-II-600. All spectra are referenced to tetramethylsilane. ESI mass spectrometry was performed with a Exactive Plus (Thermo Fisher Scientific); the mass range was 20–2000 with a nominal resolution (at m/z 200) of 140,000. Elemental analyses were carried out with a Perkin Elmer 2400II. UV-Vis and circular dichroism (CD) spectra were recorded with JASCO V-570 and J-720 spectrometers, respectively. VCD spectra were measured with a machine developed in our laboratory (H. S) with the corporation of JASCO Co. Ltd, Japan (PRESTO-S-2016 VCD-LD spectrometer). The machine is a concurrent system in combination with linear dichroism, and it is a single PEM system. The calibration was done using quarter wave-retardation and an analyzer. A $CDCl_3$ solution of the complex was injected into a cell (150 μm optical length) with BaF_2 windows. The signal was accumulated during ca. 3000 scans for each complex. The resolution was 4 cm^{-1}. Baseline correction was performed for the IR spectra by subtracting the solvent contribution. The crystal structures of Δ- and Λ-**Ru-2** were determined by the single-crystal X-ray diffraction method at 100 ± 1 K. For the collection of the diffraction data, a Rigaku Synergy diffractometer was used. The structure was solved by the direct method using the program SHELXT.[42] The refinement and all further calculations were carried out using the program SHELXL[43] with Olex2.[44] Crystallographic and experimental data are summarized in Table S1.

Sample preparation: The ruthenium complexes (**Ru-0**, **Ru-1**, and **Ru-3**) were prepared according to the previously reported procedures.[45–47]

[Ru(acac)(trop)$_2$] (**Ru-2**): [Ru(acac)$_3$] (1.04 g, 2.60 mmol) and zinc (17.7 g, 271 mmol) were added to the mixed solution of ethanol (210 ml), acetonitrile (21 ml), and water (21 ml). After a drop of aq. HCl (ca. 35%, w/w) was added to the solution, the mixture was refluxed under nitrogen atmosphere for 3 hours. After the green suspension was cooled to room temperature, it was filtered through celite and the filtrate was concentrated in vacuo. The resulting crude was washed by ethanol. The orange solid (0.614 g) corresponding to [Ru(acac)$_2$(acetonitrile)$_2$] and tropolone (0.542 g, 4.44 mmol) were added to the ethanol (300 ml). After the solution was refluxed for 1 hour, the resulting black solution was concentrated in vacuo and then purified by silica gel chromatography using toluene–acetonitrile (20 : 1 ~ 10 : 1) as an eluent, to give [Ru(acac)(trop)$_2$] as a dark-brown solid. Yield: 0.0694 g (10% yield, 0.157 mmol).

^{1}H NMR (600 MHz, $CDCl_3$): δ = -32.85 (s, 1H), -25.68 (s, 2H), -17.64 (s, 2H), -11.52 (s, 2H), -10.66 (s, 6H), 16.44 (s, 2H), 17.21 (s, 2H).

Elemental analysis: Anal. Calcd. for $C_{19}H_{17}O_6Ru$: C, 51.58; H, 3.87; Found: C, 51.75; H, 3.68. HRMS (ESI+): m/z Calcd. for $[C_{19}H_{17}O_6Ru + H]^+$: 444.0141; Found: 444.0141, m/z Calcd. for $[C_{19}H_{17}O_6Ru + Na]^+$: 465.9961; Found: 465.9961 (Fig. S1).

Enantiomeric separation: The optical resolution of **Ru-0**~**Ru-3** was performed using HPLC (Chromaster, Hitachi High-Tech Science Corp.). A chiral column (Chiralpak IA, Daicel Chemical Industries Co., Ltd.) was used for the enantiomeric separation of **Ru-1**, **Ru-2**, and **Ru-3** with a mobile phase of chloroform/hexane (2/1~3/2, v/v),[45] whereas a clay modified column (RU1-column, Shiseido Corp.) was used for **Ru-0** with a mobile phase of methanol, as previously reported.[48] The chromatograms in each enantiomeric separation are shown in Fig. S2.

DFT calculation: Unrestricted DFT and TD-DFT calculations were performed for **Ru-0**-**Ru-3** and **Ru-0**$^+$-**Ru-3**$^+$ using Gaussian 16 with cam-b3lyp functional to obtain IR, VCD and UV-Vis spectra. Structural optimization of each complex was first performed by treating them as an open shell system. The 6-311G(d) basis set was employed for the C, H, and O atoms while LANL2DZ basis set was used for Ru atom with associated ECP. The optimized structure was confirmed to be a minimum by frequency calculation. Based on the optimized structure, IR and VCD spectra were calculated, while TD-DFT calculations were performed to obtain UV-Vis spectra.

Results and discussion

Preparation, optical resolution, and absolute structure determination

[Ru(acac)$_3$] (**Ru-0**), [Ru(acac)$_2$(trop)] (**Ru-1**), and [Ru(trop$_3$)] (**Ru-3**) were prepared according to the previously reported procedures.[45–47] [Ru(acac)(trop)$_2$] (**Ru-2**) was newly obtained in a low yield (10%) when the refluxing time in the **Ru-1** synthesis was extended. The optical resolution of **Ru-0** and **Ru-1** into Δ and Λ isomers was already reported by us using HPLC with different chiral columns (See Experimental section for details).[45,49] The optical resolution of **Ru-2** and **Ru-3** was newly performed by chiral HPLC in a similar condition with that of **Ru-1**. The two enantiomers were well-separated from the baseline level as shown in Fig. S2. Single crystals of enantiomeric **Ru-2** were obtained by slow evaporation of each benzene solution. Based on single crystal X-ray diffraction analysis, the less-retained (1st) and more-retained (2nd) fractions of **Ru-2** in the chiral HPLC were determined to be Λ and Δ isomers, respectively (Fig. S3). The summary of single crystal X-ray diffraction analyses is shown in Table S1. In contrast, single crystals of enantiomeric **Ru-3** are not yet obtained at the time of writing this article, mostly because **Ru-3** gradually racemized in solution (Fig. S4).

From the comparison of elution order in HPLC of **Ru-1**, **Ru-2**, and **Ru-3**, which were performed using the same chiral column (Fig. S4), the less- and more-retained fractions of **Ru-3** were assigned to Λ and Δ isomers, respectively. However,

enantiomers of **Ru-3** show largely different ECD spectra from those of **Ru-0**. There are mainly three bands in the 250-500 nm region for Δ-**Ru-0**: 280 nm (positive), 350 nm (negative), 400-450 nm (positive) (Fig. 1). In contrast, five bands are observable in the same region for the case of the 2nd fraction of **Ru-3**: 260 nm (positive), 300 nm (negative), 350 nm (positive), 400 nm (negative) and 450 nm (positive) (Fig. 1). The bands around 350 nm and 400 nm show opposite signs. Hence, it was difficult to determine the absolute configuration of **Ru-3** just from the comparison of the ECD spectrum with that of **Ru-0**, for which detailed ECD studies were previously performed.[50,51] In contrast, the systematic comparison of ECD spectra of **Ru-0**, **Ru-1**, **Ru-2**, and **Ru-3** series indicates their organized changes (Fig. 1). For example, the ECD signals around 350 nm gradually change from negative to positive with the increase of trop ligand numbers, whereas those around 400 nm gradually change from positive to negative as the number of trop ligands increases. Based on the systematic comparison, the 1st and 2nd fractions of **Ru-3** are deduced to be Λ and Δ isomers, respectively, consistent with the elution order in HPLC. Each ECD spectrum of Δ and Λ isomers of **Ru-0**, **Ru-1**, **Ru-2**, and **Ru-3** is shown in Fig. S5.

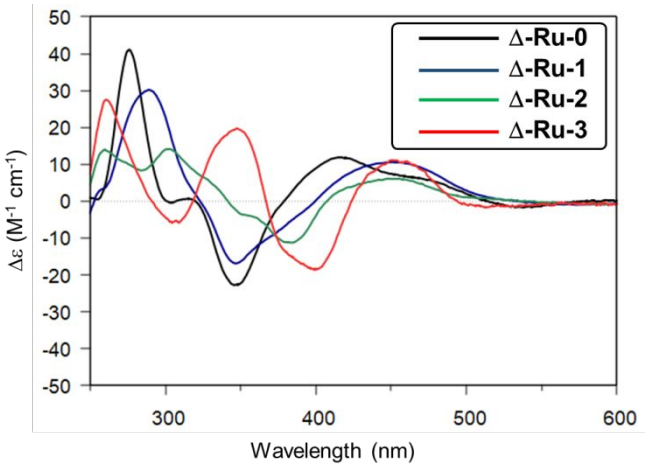

Fig. 1 Experimental ECD spectra of Δ isomers of **Ru-0**, **Ru-1**, **Ru-2**, and **Ru-3**. The 2nd fraction in the HPLC chromatogram of **Ru-3** was assigned to Δ isomer.

VCD analysis

To confirm the absolute configuration of **Ru-3**, the vibrational circular dichroism (VCD) and IR spectra of the enantiomeric **Ru-0**, **Ru-1**, **Ru-2**, and **Ru-3** were further measured in deuterated chloroform solution (Fig. 2). The vertical axes in the spectra of **Ru-0**, **Ru-1**, and **Ru-2** corresponds to molar epsilon, while that of **Ru-3** is arbitrary due to the racemization in solution. All the complexes show relatively strong VCD signals, as often observed in metal-containing materials.[52–55] The VCD spectra of two enantiomers in each complex were in the relation of mirror-image, confirming the reliability of the measurements. **Ru-0** shows a characteristic two bands in the region from 1300 to 1400 cm^{-1} as previously reported in detail by Sato.[56–60] The band in the higher frequency in the 1300~1400 cm^{-1} region was attributed to the C=O stretching band in all-in-phase, while that in the lower frequency was attributed to the out-of-phase stretches. Similar strong signals are also observed in the 1300~1400 cm^{-1} region in both **Ru-2** and **Ru-3**, whereas the signs of the bands were opposite from that of **Ru-0**. In addition, the VCD signals of **Ru-1** in this region are weak. The signals in the 1300-1400 cm^{-1} region appear to be inverted as the number of trop ligands increases.

The experimental VCD and IR spectra were then compared with DFT calculated spectra. The calculations were performed using Gaussian 16 with ucam-b3lyp functional. Each optimized structure was confirmed to be a minimum by frequency calculation. The calculated VCD spectra match well enough with those of experimental spectra in all complexes. Also in the calculated spectra, the major signals around 1300-1350 cm^{-1} region (A_1~D_1) are inverted as the number of trop ligands increases (Fig. 3). The vibration modes of the calculated major peaks were further analyzed (Fig. 4). For Λ-**Ru-0**, the positive band around 1330 cm^{-1} (marked as A_1) and negative band around 1400 cm^{-1} (A_2) are assigned to the out-of-phase and all-in-phase stretches of the six CO, respectively, consistent with previous reports.[56–60] In contrast, for the case of **Ru-3**, the major peak around 1350 cm^{-1} marked as D_1 in Fig. 4 is attributed to the asymmetric stretching of C=O group in trop ligands. The vibration modes of the signals around 1330 cm^{-1} in **Ru-1** and **Ru-2** are also attributed to the combination of asymmetric stretching of acac and trop ligands. In this sense, the sign inversion of the calculated VCD signals (A_1~D_1) is attributed to the opposite signs of different vibration modes of acac and trop ligands (Figs. 3,4). The experimental signals in **Ru-1** are supposed to be weak because of the canceling out of vibration modes of acac and trop ligands. The consistency in the experimental and calculated VCD spectra also supports the ΔΛ absolute configuration of **Ru-3** proposed by HPLC and ECD studies. The experimental and calculated IR spectra are shown in Fig. S6.

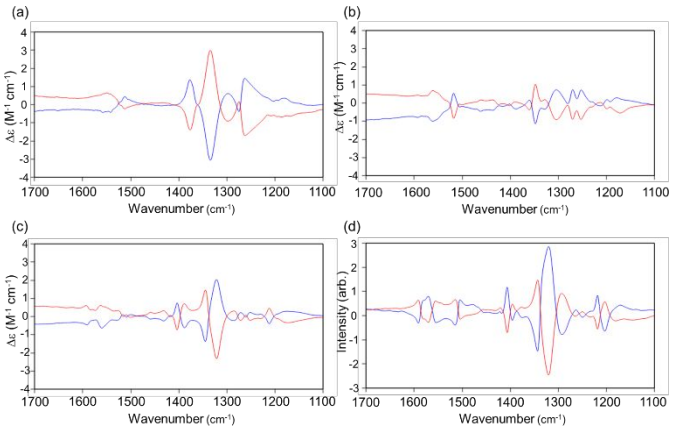

Fig. 2 The observed VCD spectra for two antipodal pairs of (a) **Ru-0**, (b) **Ru-1**, (c) **Ru-2**, and (d) **Ru-3**. Blue and red lines correspond to Δ and Λ isomers, respectively.

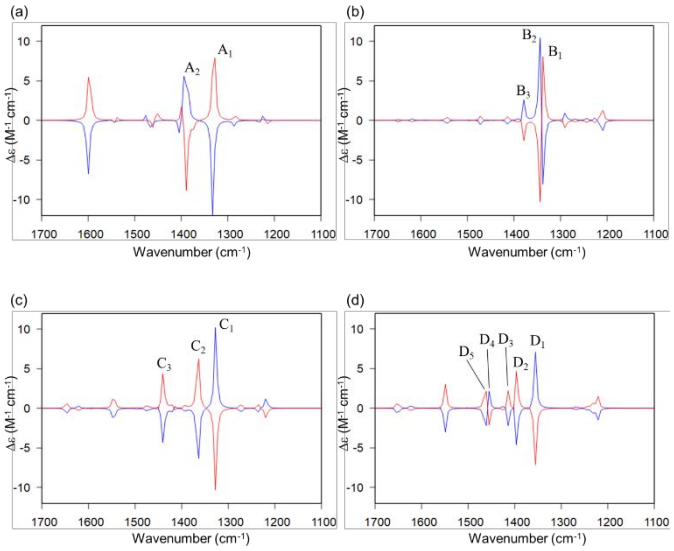

Fig. 3 DFT-calculated VCD spectra for two antipodal pairs of (a) **Ru-0**, (b) **Ru-1**, (c) **Ru-2**, and (d) **Ru-3** (Scale = 0.98). Blue and red lines correspond to Δ and Λ isomers, respectively.

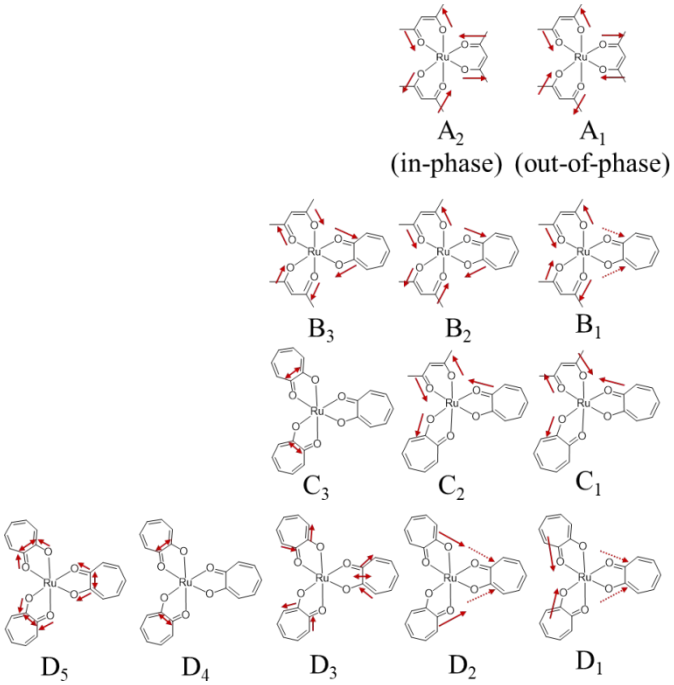

Fig. 4 Major vibration modes corresponding to the signals in Fig. 3.

Chemical oxidation and ECD changes upon oxidation

We previously reported that one-electron oxidations of **Ru-0**, **Ru-1**, and **Ru-3** proceed via electrochemical oxidation or chemical oxidation by using ceric(IV) ammonium nitrate (CAN) as an oxidant (Figs. S7,S8).[33] Here, we also examined the chemical oxidation of **Ru-2**. Fig. 5 shows the drastic spectral change of **Ru-2** upon the addition of ca. 1 equiv. of CAN. The newly appeared absorption around 800 nm in the oxidized **Ru-2** is attributed to the excitation from the orbitals delocalized over the ruthenium and trop ligands according to the TD-DFT calculations of **Ru-2** and **Ru-2**$^+$ (Fig. S9,S10 and Table S2). The UV-Vis-NIR spectra of the four ruthenium complexes are similar in each oxidized state(Fig. S7), supporting that **Ru-2** is also one-electron oxidized to **Ru-2**$^+$. After the addition of CAN, the spectrum attributed to **Ru-2**$^+$ gradually returned to that of **Ru-2** with isosbestic points at 362 and 475 nm, except for the wavelengths shorter than 450 nm where the absorption attributed to CAN co-exists. The successive change supports the reversible redox reaction between **Ru-2** and **Ru-2**$^+$.

The ECD spectra of the mono-oxidized complexes, **Ru-0**$^+$, **Ru-1**$^+$, **Ru-2**$^+$, and **Ru-3**$^+$, were then measured in acetonitrile solution (Fig. 6). In every case, the in-situ oxidized complexes show different ECD spectra from corresponding neutral complexes. The ECD change was explicit in the wavelengths longer than 450 nm for the cases of **Ru-1** and **Ru-2**; new ECD peaks appeared around 475-500 nm and 600 nm. Further, the resultant ECD spectra of two enantiomers of the oxidized complexes are in the relation of mirror-image (Fig. S11), confirming the reproducibility of the ECD changes. The scan speed was set to 200 nm/min except for **Ru-0**, in which the scan rate was set to 500 nm/nm, because **Ru-0**$^+$ returned to **Ru-0** within ca. two minutes in acetonitrile.[33]

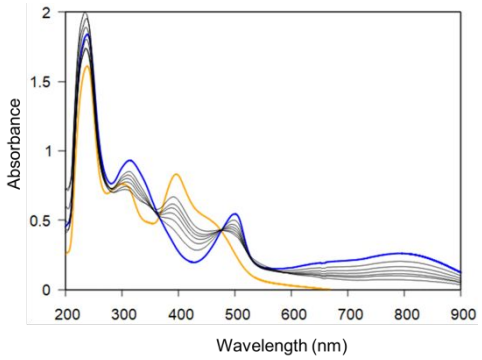

Fig. 5 UV-Vis-NIR spectra of **Ru-2** (orange line) in CH_3CN (ca. 6.7×10^{-5} M) and **Ru-2**$^+$ (blue line), which was in-situ prepared by the addition of 1 equiv. of CAN. The spectral change was further monitored for 3 hours (black lines).

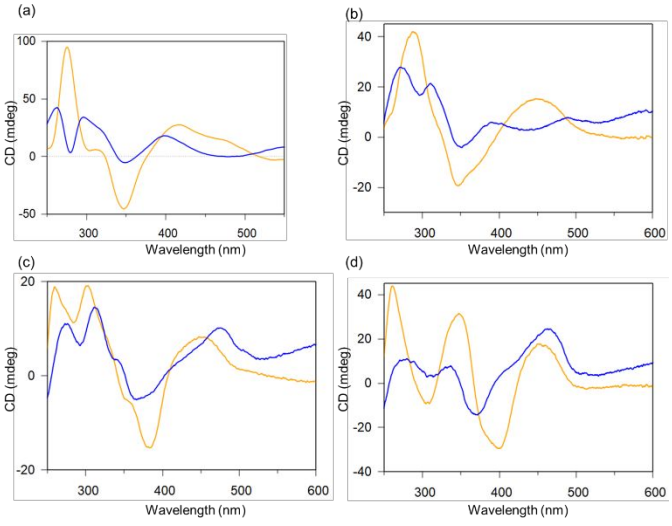

Fig. 6 ECD spectra of Δ isomers of (a) **Ru-0**, (b) **Ru-1**, (c) **Ru-2**, and (d) **Ru-3** before and after the oxidation. Orange and blue lines correspond to neutral and oxidized complexes, respectively. The scan speed is 200 nm/min, except for **Ru-0**, in which the scan speed wase set to 500 nm/min.

The ECD spectra of Δ isomers of mono-oxidized metal complexes are superimposed (Fig. 7(a)). As the number of trop ligands increases, two characteristic changes are observed; (1) the sign of the CD signals in the 350~400nm region changes from positive to negative and (2) new positive signals appear around 460 nm. The TD-DFT study of **Ru-0**$^+$, **Ru-1**$^+$, **Ru-2**$^+$, and **Ru-3**$^+$ was then performed. Although the peak positions in the calculated spectra are shifted by ca. 100 nm toward the shorter wavelength, the systematic change of the four complexes (shown by grey arrows in Fig. 7) was predicted correctly.

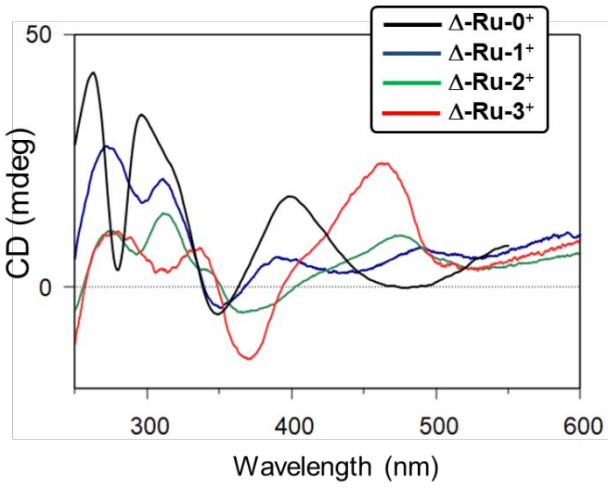

Fig. 7 Experimental ECD spectra of Δ isomers of mono-oxidized ruthenium complexes, which were in-situ prepared by the addition of CAN.

All the complexes investigated in this study, **Ru-0**~**Ru-3**, exhibited ECD changes upon the oxidation. In particular, **Ru-3** shows largely different ECD spectrum upon oxidation, indicating the usability as a redox-triggered ECD switching material. In contrast, **Ru-3** gradually racemized in solution (Fig. S4). The racemization of **Ru-3** is fairly fast as a tris-chelate ruthenium complex, to the best of our knowledge. **Ru-0** and **Ru-1** were enantiomerically stable. Besides, the racemization speed of **Ru-2** was quite slow compared to that of **Ru-3** (Fig. S4). The presence of acac ligand appears to avoid the racemization. According to our single crystal XRD study of racemic **Ru-3**,[33] O-Ru-O angle in **Ru-3** is ca. 80°, fairly small compared to ca. 93° of O-Ru-O angle in **Ru-0**. Such a small O-Ru-O angle in **Ru-3** may lead to the flexible structural conversion between Δ and Λ isomers and racemization. In contrast, the introduction of trop ligand was effective to improve the stability of mono-oxidized state. As the number of trop ligands increases, the lifetime of the mono-oxidized complexes was extended (Fig. S12).[33] In this sense, heteroleptic complexes such as **Ru-1** and **Ru-2** are currently promising as a redox-triggered ECD switch in terms of the balance of the lifetime of the oxidized states and anti-racemization.

The modification of a trop ligand may be an approach to utilize [Ru(trop)$_3$] framework as a chiroptical switch. The introduction of bulky substituents such as at 3, 7-positions of trop may inhibit the racemization of the resulting tris-chelate complexes. The synthesis and redox properties of ruthenium complexes with such bulky tropolone derivatives are now under investigation by our group.

Conclusions

Four ruthenium complexes bearing acac and trop ligands, [Ru(acac)$_3$] (**Ru-0**), [Ru(acac)$_2$(trop)] (**Ru-1**), [Ru(acac)(trop)$_2$] (**Ru-2**), and [Ru(trop)$_3$] (**Ru-3**), have been prepared and optically resolved into Δ and Λ isomers by using chiral HPLC. After the absolute configurations have been determined by the systematic comparison of chromatographic charts and ECD and VCD spectra, the chiroptical properties of each complex in the neutral and mono-oxidized states have been investigated. All the complexes showed ECD changes upon the mono-electron oxidation. The introduction of trop ligands was effective in terms of stabilizing the oxidized state. However, **Ru-3** gradually racemized in solution. Because the racemization of **Ru-2** was quite slow, the presence of an acac ligand was supposed to suppress the racemization. In terms of the balance of the lifetime of oxidized species and racemization rate, the heteroleptic complexes **Ru-1** and **Ru-2** are concluded to be appropriate as a ECD switch.

Author Contributions

JY led the experiments, provided experimental guidance and financial support, and wrote the manuscript. KY and KT conducted the experiments, collected, and processed the experimental data. HY helped with XRD experiment. HS led the VCD experiments and analysis.

Conflicts of interest

There are no conflicts to declare.

Acknowledgements

This work was financially supported by the Japan Society for the Promotion of Science (JSPS) KAKENHI Grant (JP17H03044 and JP19K05508), the Japan Science and Technology Agency (JST) MIRAI Grant (JPMJMI18GC). The computations were performed at the Research Center for Computational Science, Okazaki, Japan.

References

1 Y. Kasahara, Y. Hoshino, M. Kajitani and K. Shimizu, *Organometallics*, 1992, **11**, 1968–1971.
2 C. Remenyi and M. Kaupp, *J. Am. Chem. Soc.*, 2005, **127**, 11399–11413.
3 F. Ehret, M. Bubrin, S. Zalis, J. L. Priego, R. Jimmenez-Aparicio and W. Kaim, *Chem. Eur. J.*, 2015, **21**, 15163–15166.
4 P. Mondal, A. Das and G. K. Lahiri, *Inorg. Chem.*, 2016, **55**, 1208–1218.
5 S. Maji, B. Sarkar, S. M. Mobin, J. Fiedler, F. A. Urbanos, R. Jimenez-Aparicio, W. Kaim and G. K. Lahiri, *Inorg. Chem.*, 2008, **47**, 5204–5211.

6 S. Ghumaan, B. Sarkar, S. Maji, V. G. Puranik, W. Kaim and G. K. Lahiri, *Chem. Eur. J.*, 2008, **14**, 10816–10828.
7 D. Kalinina, C. Dares, H. Kaluarachchi, P. G. Potvin and A. B. P. Lever, *Inorg. Chem.*, 2008, **47**, 10110–10126.
8 D. Kumbhakar, B. Sarkar, S. Maji, S. M. Mobin, J. Fiedler, F. a Urbanos, R. Jiménez-Aparicio, W. Kaim and G. K. Lahiri, *J. Am. Chem. Soc.*, 2008, **130**, 17575–17583.
9 T. Kundu, S. M. Mobin and G. K. Lahiri, *Dalton Trans.*, 2010, **39**, 4232–4242.
10 A. Das, T. Scherer, S. Maji, T. K. Mondal, S. M. Mobin, F. A. Urbanos, R. Jiménez-Aparicio, W. Kaim and G. K. Lahiri, *Inorg. Chem.*, 2011, **50**, 7040–7049.
11 S. Roy, B. Sarkar, H.-G. Imrich, J. Fiedler, S. Záliš, R. Jimenez-Aparicio, F. A. Urbanos, S. M. Mobin, G. K. Lahiri and W. Kaim, *Inorg. Chem.*, 2012, **51**, 9273–9281.
12 P. Mondal, F. Ehret, M. Bubrin, A. Das, S. M. Mobin, W. Kaim and G. K. Lahiri, *Inorg. Chem.*, 2013, **52**, 8467–8475.
13 G. H. Allen, R. P. White, D. P. Rillema and T. J. Meye, *J. Am. Chem. Soc.*, 1984, **106**, 2613–2620.
14 C. Moucheron, A. Kirsch-De Mesmaeker and S. Choua, *Inorg. Chem.*, 1997, **36**, 584–592.
15 L. S. Sapochak, A. Padmaperuma, N. Washton, F. Endrino, G. T. Schmett, J. Marshall, D. Fogarty, P. E. Burrows and S. R. Forrest, *J. Am. Chem. Soc.*, 2001, **123**, 6300–6307.
16 L. Wang, H. Yin, P. Cui, M. Hetu, C. Wang, S. Monro, R. D. Schaller, C. G. Cameron, B. Liu, S. Kilina, S. A. McFarland and W. Sun, *Dalton Trans.*, 2017, **46**, 8091–8103.
17 Q. Zhao, N. Katyal, I. D. Seymour, G. Henkelman and T. Ma, *Angew. Chemie*, 2019, **131**, 12683–12687.
18 L. B. Backman, A. Rautiainen, M. Lindblad, O. Jylhä and A. O. I. Krause, *Appl. Catal. A Gen.*, 2001, **208**, 223–234.
19 D. L. Murphy, M. R. Malachowski, C. F. Campana and S. M. Cohen, *Chem. Commun.*, 2005, 5506–5508.
20 J. Crassous, *Chem. Soc. Rev.*, 2009, **38**, 830–845.
21 E. Meggers, *Eur. J. Inorg. Chem.*, 2011, **2011**, 2911–2926.
22 C. Wang, L.-A. Chen, H. Huo, X. Shen, K. Harms, L. Gong and E. Meggers, *Chem. Sci.*, 2015, **6**, 1094–1100.
23 J. W. Canary, *Chem. Soc. Rev.*, 2009, **38**, 747–756.
24 J. R. Brandt, L. Pospíšil, L. Bednárová, R. C. Da Costa, A. J. P. White, T. Mori, F. Teplý and M. J. Fuchter, *Chem. Commun.*, 2017, **53**, 9059–9062.
25 D. Schweinfurth, M. Zalibera, M. Kathan, C. Shen, M. Mazzolini, N. Trapp, J. Crassous, G. Gescheidt and F. Diederich, *J. Am. Chem. Soc.*, 2014, **136**, 13045–13052.
26 M. Hasegawa, K. Kobayakawa, H. Matsuzawa, T. Nishinaga, T. Hirose, K. Sako and Y. Mazaki, *Chem. Eur. J.*, 2017, **23**, 3267–3271.
27 M. Kos, R. Rodriguez, J. Storch, J. Sykora, E. Caytan, M. Cordier, I. Cisařova, N. Vanthuyne, J. A. G. Williams, J. Žadny, V. Cirkva and J. Crassous, *Inorg. Chem.*, 2021, **60**, 11838–11851.
28 N. Saleh, N. Vanthuyne, J. Bonvoisin, J. Autschbach, M. Srebro-Hooper and J. Crassous, *Chirality*, 2018, **30**, 592–601.
29 M. Cortijo, C. Viala, T. Reynaldo, L. Favereau, I. Fabing, M. Srebro-Hooper, J. Autschbach, N. Ratel-Ramond, J. Crassous and J. Bonvoisin, *Inorg. Chem.*, 2017, **56**, 4555–4567.
30 S. Zahn and J. W. Canary, *J. Am. Chem. Soc.*, 2002, **124**, 9204–9211.
31 J. Yoshida, K. Kuwahara and H. Yuge, *J. Organomet. Chem.*, 2014, **756**, 19–26.
32 J. Yoshida, K. Kuwahara, K. Suzuki and H. Yuge, *Inorg. Chem.*, 2017, **56**, 1846–1856.
33 J. Yoshida, K. Tateyama and H. Yuge, *Dalton Trans.*, 2020, **49**, 2102–2111.
34 F. A. Cotton and R. H. Holm, *J. Am. Chem. Soc.*, 1960, **82**, 2979–2983.
35 T. S. Davis, J. P. Fackler and M. J. Weeks, *Inorg. Chem.*, 1968, **7**, 1994–2002.
36 M. Haga, E. S. Dodsworth and A. B. P. Lever, *Inorg. Chem.*, 1986, **25**, 447–453.
37 T. Wada, K. Tsuge and K. Tanaka, *Inorg. Chem.*, 2001, **40**, 329–337.
38 J. T. Muckerman, D. E. Polyansky, T. Wada, K. Tanaka and E. Fujita, *Inorg. Chem.*, 2008, **47**, 1787–1802.
39 J. L. Boyer, J. Rochford, M.-K. Tsai, J. T. Muckerman and E. Fujita, *Coord. Chem. Rev.*, 2010, **254**, 309–330.
40 W. Kaim, *Inorg. Chem.*, 2011, **50**, 9752–9765.
41 D. L. J. Broere, R. Plessius and J. I. van der Vlugt, *Chem. Soc. Rev.*, 2015, **44**, 6886–6915.
42 G. M. Sheldrick, *Acta Cryst. A*, 2015, **71**, 3–8.
43 G. M. Sheldrick, *Acta Cryst. C*, 2015, **71**, 3–8.
44 O. V. Dolomanov, L. J. Bourhis, R. J. Gildea, J. A. K. Howard and H. Puschmann, *J. Appl. Crystallogr.*, 2009, **42**, 339–341.
45 J. Yoshida, K. Kuwahara, S. Tamura, H. Yuge and G. Watanabe, *Mol. Cryst. Liq. Cryst.*, 2017, **647**, 179–185.
46 T. Koiwa, Y. Masuda, J. Shono, Y. Kawamoto, Y. Hoshino, T. Hashimoto, K. Natarajan and K. Shimizu, *Inorg. Chem.*, 2004, **43**, 6215–6223.
47 A. Endo, K. Shimizu, G. P. Satô and M. Mukaida, *Chem. Lett.*, 1984, **13**, 437–440.
48 S. Kashiwara, M. Takahashi, M. Nakata, M. Taniguchi and A. Yamagishi, *J. Mater. Chem.*, 1998, **8**, 2253–2257.
49 J. Yoshida, S. Tamura, K. Hoshino, H. Yuge, H. Sato, A. Yamazaki, S. Yoneda and G. Watanabe, *J. Phys. Chem. B*, 2018, **122**, 10615–10626.
50 T. Kobayashi, Y. Nishina, K. Shimizu and G. P. Satô, *Chem. Lett.*, 1988, **17**, 1137–1140.
51 H. Kobayashi, H. Matsuzawa, Y. Kaizu and A. Ichida, *Inorg. Chem.*, 1987, **26**, 4318–4323.
52 Y. He, X. Cao, L. A. Nafie and T. B. Freedman, *J. Am. Chem. Soc.*, 2001, **123**, 11320–11321.
53 C. J. Barnett, A. F. Drake, R. Kuroda, S. F. Mason and S. Savage, *Chem. Phys. Lett.*, 1980, **70**, 8–10.
54 L. A. Nafie, *J. Phys. Chem. A*, 2004, **108**, 7222–7231.
55 L. Arrico, G. Angelici and L. Di Bari, *Org. Biomol. Chem.*, 2017, **15**, 9800–9803.
56 H. Sato, T. Taniguchi, A. Nakahashi, K. Monde and A. Yamagishi, *Inorg. Chem.*, 2007, **46**, 6755–6766.
57 H. Sato, Y. Mori, Y. Fukuda and A. Yamagishi, *Inorg. Chem.*, 2009, **48**, 4354–4361.

58 H. Mori, A. Yamagishi and H. Sato, *J. Chem. Phys.*, 2011, **135**, 084506.
59 H. Sato, Y. Mori, T. Kitazawa and A. Yamagishi, *Dalton Trans.*, 2013, **42**, 232–237.
60 H. Sato, F. Sato and A. Yamagishi, *Inorganics*, 2018, **6**, 70.